Published in final edited form as:
Int J Pharm. 2013 July 15; 451(0): 76–91. doi:10.1016/j.ijpharm.2013.04.045.

Hydrogel-forming Microneedle Arrays Exhibit Antimicrobial Properties: Potential for Enhanced Patient Safety

Ryan F. Donnelly[a,*], **Thakur Raghu Raj Singh**[a], **Ahlam Zaid Alkilani**[a,c], **Maelíosa T.C. McCrudden**[a], **Conor O'Mahony**[b], **Keith Armstrong**[d], **Nabla McLoone**[e], **Prashant Kole**[a], and **A. David Woolfson**[a]

[a]School of Pharmacy, Queens University Belfast, Medical Biology Centre, 97 Lisburn Road, Belfast BT9 7BL, Northern Ireland, UK [b]Tyndall National Institute, Lee Maltings, Prospect Row, Cork, Ireland [c]School of Pharmacy, Zarqa University, Zarqa 132222, Jordan [d]Royal Victoria Hospital, Grosvenor Road, BT12 6BA, Belfast, Northern Ireland, UK [e]Antrim Area Hospital, 45 Bush Road, Antrim BT41 2RL, Northern Ireland, UK

Abstract

We describe, for the first time, the microbial characterisation of hydrogel-forming polymeric microneedle arrays and the potential for passage of microorganisms into skin following microneedle penetration. Uniquely, we also present insights into the storage stability of these hydroscopic formulations, from physical and microbiological viewpoints, and examine clinical performance and safety in human volunteers. Experiments employing excised porcine skin and radiolabelled microorganisms showed that microorganisms can penetrate skin beyond the *stratum corneum* following microneedle puncture. Indeed, the numbers of microorganisms crossing the *stratum corneum* following microneedle puncture was greater than 10^5 cfu in each case. However, no microorganisms crossed the epidermal skin. When using a 21G hypodermic needle, more than 10^4 microorganisms penetrated into the viable tissue and 10^6 cfu of *C. albicans* and *S. epidermidis* completely crossed the epidermal skin in 24 h. The hydrogel-forming materials contained no microorganisms following de-moulding and exhibited no microbial growth during storage, while also maintaining their mechanical strength, apart from when stored at relative humidities of 86%. No microbial penetration through the swelling microneedles was detectable, while human volunteer studies confirmed that skin or systemic infection is highly unlikely when polymeric microneedles are used for transdermal drug delivery. Since no pharmacopoeial standards currently exist for microneedle-based products, the exact requirements for a proprietary product based on hydrogel-forming microneedles are at present unclear. However, we are currently working towards a comprehensive specification set for this microneedle system that may inform future developments in this regard.

[*]Corresponding author Dr Ryan F. Donnelly Reader in Pharmaceutics School of Pharmacy, Queens University Belfast, Medical Biology Centre, 97 Lisburn Road, Belfast BT9 7BL, UK Tel: +44 (0) 28 90 972 251 Fax: +44 (0) 28 90 247 794 r.donnelly@qub.ac.uk.

Europe PMC Funders Author Manuscripts

Keywords

Microneedle; microorganism; stability; pharmacopoeial standards

Introduction

Despite the limited number of drugs amenable to administration across the skin, due to the excellent barrier properties of the *stratum corneum*, the worldwide transdermal product market is predicted to grow from $20 billion to $32 billion by 2015 (PMPN, 2012; prweb, 2012). The major growth drivers are: greater patient acceptance leading to wider market penetration, lowered development costs and introduction of novel technologies instigating market growth. A key area for development is transdermal delivery of therapeutic peptides and proteins. There are over 100 biotechnology-derived medicines marketed, covering 9 major therapeutic areas, now representing approximately 15% of all prescriptions in the UK. A major challenge to successful clinical use of these hydrophilic, high molecular weight "biotech" molecules is drug delivery. Due to enzymatic breakdown and poor GI absorption, the parenteral route is presently the only option. Microneedle (MN) based transdermal systems have the potential to effectively overcome this problem and can also eliminate transdermal dosing variability, due to inter-patient differences in skin thickness and intra-patient skin variability, as they completely bypass the skin barrier. Thus, such systems could greatly enhance market size by removing dependence of efficient transdermal transport on drug physicochemical properties, allowing a much greater range of drugs to be delivered transdermally. In fact, conventional MN arrays have already successfully delivered oligonucleotides, desmopressin, DNA, vaccines, insulin and human growth hormone *in vivo*. Indeed, a new report from Greystone Associates, Microneedles in Medicine: Technology, Devices, Markets and Prospects, puts the MN drug delivery market at just under $400 million globally by 2012 (Greystone Associates, 2012). Since MN are frequently targeted not only to the $20 billion transdermal drug delivery and $25 billion global vaccine markets, but also to the $120 billion global biologics market, significant further growth is anticipated. While the first two microneedle-based products, just recently marketed, Soluvia® and Micronjet® , are based on metal and silicon MN, respectively, the current trend in MN-based research has involved recognition of the dubious biocompatibility of silicon and the potential for inappropriate reuse of silicon or metal microneedles, which remain fully intact after removal from a patient's skin. Consequently, much recent effort has focussed on MN prepared from FDA-approved biocompatible polymers (Donnelly *et al*., 2012a). Initially, such systems were prepared from hot polymer/carbohydrate melts. However, the high processing temperatures lead to degradation of the biomolecules cargoes (Donnelly *et al*., 2009a). Accordingly, an increasing emphasis has been placed on MN formulated from aqueous polymer gels (Donnelly *et al*., 2012a; Migalska *et al*., 2011). We have recently described novel hydrogel-forming MN arrays, prepared under ambient conditions that contain no drug themselves (Donnelly *et al*., 2012b). Instead, they rapidly imbibe skin interstitial fluid upon insertion to form continuous, unblockable conduits between the dermal microcirculation and an attached patch-type drug reservoir. In so-doing, we have overcome one of the noted limitations of dissolving polymeric MN, in that delivered doses of biomolecules are no longer limited to what can be loaded into the needles themselves

Europe PMC Funders Author Manuscripts

(Donnelly *et al*., 2012b; Migalska *et al*., 2011). Such hydrogel-forming MN initially act simply as a tool to pierce the *stratum corneum* barrier and then function as a rate-controlling membrane (Figure 1), allowing sustained delivery of high doses of biomolecules. Importantly, such MN are removed intact from skin, leaving no polymer residue behind, but are sufficiently softened, even after 1 minute of skin insertion to preclude reinsertion, thus further reducing the risk of transmission of infection (Donnelly *et al*., 2012b).

MN devices are not equivalent to conventional transdermal patches, in that they are not simply applied to the skin surface. Rather MN function principally by breaching the skin's protective *stratum corneum* barrier and often penetrate into the viable epidermis and dermis (Donnelly *et al*., 2012a; Donnelly *et al*., 2010). Such areas of the body are normally sterile. Accordingly, it is imperative that MN do not contain microbial loads sufficient to cause skin or systemic infection. It is also important that bioburden be minimised to avoid immune stimulation, especially considering the rich immune cell population in the viable epidermis and dermis (Al-Zahrani *et al*., 2012). In this study, we investigate, for the first time, the microbial content of polymeric MN and the potential for passage of microorganisms into skin following MN penetration. Uniquely, we also present insights into the storage stability of these hydroscopic formulations, from physical and microbiological viewpoints, and examine clinical performance and safety in human volunteers.

Materials and Methods

Chemicals and microorganisms

Gantrez® AN-139, a copolymer of methyl vinyl ether and maleic anhydride (PMVE/MAH, M_w = 1,080,000) was a gift from ISP Corp. Ltd (Guildford, U.K). Polyethylene glycol (PEG, molecular weight 10,000 daltons) was purchased from Sigma-Aldrich (Steinheim, Germany, U.K). Poly(ester) film, one-side siliconised, release liner, FL2000 PET 75 1S, was obtained from Rexam Release B.V. (Apeldoom, The Netherlands). Glisseal® N vacuum grease was purchased from Borer chemie (Zuchwil, Switzerland). Silastic® 9280/60E silicone elastomer was obtained from Dow Corning (Wiesbaden, Germany). Resealable plastic bags (101 × 140 mm) were obtained from Agar Scientific (Essex, UK). Millipore water was used throughout the study. A 1.0 mCi vial of tritium-labelled [5′-^{3}H] thymidine was purchased form GE Healthcare, Buckinghamshire, UK. All other chemicals used were of analytical reagent grade. *Escherichia coli* ATCC® 11303, *Staphylococcus aureus* NCTC 10788, *Pseudomonas aeruginosa* NCIMB 8626, *Candida albicans* NCPF 3179 and *Aspergillus brasiliensis* IMI 149007 were obtained from LCG Standards, Middlesex, UK

Fabrication of master template silicon MN arrays

Silicon MN arrays to be used as master templates in micromoulding of hydrogel-forming arrays were microfabricated using a previously-reported approach (Donnelly *et al*., 2009a). The aspect ratio of these MNs was 3:2 (height:base diameter) with a height of 280 μm, a diameter of 240 μm at the base and an interspacing of 750 μm between rows of MNs, as shown in Figure 2.

Fabrication of hydrogel-forming MN arrays

Using the above silicon MN arrays as master templates, silicone elastomer micromoulds were prepared, as described previously (Donnelly *et al*., 2009a). In order to fabricate the hydrogel-forming MNs, approximately 10 g of aqueous blends of PEG-PMVE/MA gels (15% w/w PMVE/MA & 7.5% w/w PEG 10, 000) were carefully poured into the formed silicone moulds and the aluminium lid screwed on (Figure 3) and centrifuged for 15 minutes at 3500 rpm. After centrifugation, PEG-PMVE/MA MNs were dried at room temperature for 48 hours. The micromould containing the formed MN was then heated at 80°C for 24 hours to induce ester-based crosslinking between PEG and PMVE/MA. Upon cooling, the silicone moulds containing the PEG-PMVE/MA MN arrays were removed from the aluminium holder, as shown in Figure 3. The side-walls of the PEG-crosslinked PMVE/MA MN arrays (Figure 3D) were carefully removed using a hot scalpel blade (Figure 3E).

Mechanical testing of MN arrays

Hydrogel-forming MN were subjected to standard mechanical tests using a TA-XT2 Texture Analyser (Stable Microsystems, Haslemere, UK) in compression mode, as described previously (Donnelly *et al*., 2011).

Stability studies

To evaluate the storage stability of the PEG-crosslinked PMVE/MA MN arrays, the MN arrays or their base-plates (with no MN) were exposed to different relative humidities (RHs) and stored in a temperature controlled environment (20.0 ± 2.0°C) for three weeks. The three different RH selected were 0%, 43%, and 86%. The RHs of 43% and 86% represented the bench-top RH of the laboratory and the average outdoor RH in the United Kingdom (BBC, 2008), respectively. As a control, MN arrays were also stored at 0% RH. Saturated solutions of potassium carbonate and potassium chloride were used to create RHs of 43% and 86%, respectively. Samples of MN base-plates and MN arrays of each type of formulation was placed inside sealed chambers, containing either saturated salt solutions (43% & 86% RH) or purge nitrogen for maintaining 0% RH. Samples were removed at predetermined intervals of 0, 3, 7, 14 and 21 days and analyzed for folding endurance (FE), percentage water content, glass transition temperature (T_g), and axial fracture force, as detailed below. Microbial content was also determined at all storage times for each of the storage conditions using the methods described below.

Folding endurance

Hydrogel-forming MN base-plates were evaluated for their folding endurance (FE, a test of flexibility of polymeric materials, Ubaidulla *et al*., 2007). Briefly, FE was determined by repeatedly folding the base-plate (1.0 × 1.0 cm) at the same place until it broke. Crosslinked MN base-plates which broke after a single fold were considered to have a FE value of zero and, therefore, were considered to be hard/glassy. MN base-plates with a FE of one or more were considered soft and rubbery in nature. This test was used to determine if the MN base-plates remain hard/glassy in nature during stability studies. At least three measurements were taken and mean values were reported.

Thermal analysis

Change in state of the hydrogel-forming MN base-plates from hard/glassy (T_g above room temperature) to soft/rubbery (T_g below room temperature) were investigated by differential scanning calorimetry (DSC). DSC studies of MN base-plates were carried out with a DSC Q100 (TA Instruments Ltd, Herts, UK). Sample weights of 5.0–10.0 mg were sealed in non-hermetic-type aluminum pans and ramped at a heating rate of 10.0°C/min in nitrogen at a flow rate of 50.0 mL/min. The DSC was calibrated with the melting temperature of indium (156.6°C). The glass transition temperature (T_g) of the MN base-plates, removed from storage at different time intervals, was determined as the mid-span temperature of the step change in the heat-capacity curve. The percentage water content of the MN base-plates was determined with a Q500 thermogravimetric analyzer (TGA). Samples of 5.0–10.0 mg were heated from ambient temperature to 200°C at a heating rate of 5°C/min. Nitrogen flow rates of 40.0 mL min^{-1} (balance purge gas) and 60.0 mL min^{-1} (sample purge gas) were maintained for all samples. The data from both the DSC and thermogravimetric analysis experiments were analyzed with TA Instruments Universal Analysis 2000 software, version 4.4A. At least three measurements were taken, for both DSC and TGA studies and a mean was determined in each case.

Axial fracture force

Samples of MN arrays were also evaluated for axial fracture forces. The axial fracture force of the MN arrays was determined, at a defined force of 0.2 N $needle^{-1}$, using the Texture Analyser and the methods described previously (Donnelly *et al*., 2011).

Microbiological examination of hydrogel MN materials

We subjected the hydrogel MN material to an enumeration of microorganisms test, conducted in accordance with the harmonized European Pharmacopoeial test (*PhEur*) (*Ph Eur*, 2007). The PhEur test 2.6.12 was performed to determine the “total aerobic microbial count” (TAMC) and “total yeasts and moulds counts” (TYMC) for the aqueous hydrogel mixture and crosslinked MN. For this general microbial content test, hydrogel samples, both the aqueous gel used in MN formulation (5 g) and the crosslinked MN (10 MN), were extracted in a buffered sodium chloride–peptone solution (500 ml) at pH 7 for 30 min. Under sterile conditions, 0.1ml of the sample was spread over the surface of a liquefied agar medium suitable for cultivation of bacteria (Casein soya bean digest agar) or fungi (Sabouraud glucose agar). The plates were then incubated at 30-35°C (20-25°C for fungi) for 5 days, unless reliable counts were obtained in a shorter time. Growth of colonies indicates the possible presence of microorganisms, according to *PhEur* standards (*Ph Eur*, 2007). To determine the presence of specific microorganisms, namely *Pseudomonas aeruginosa* and *Staphylococcus aureus*, a cetrimide agar plate and mannitol salt agar plate were used. The results were reported in triplicate.

Since it is possible that microorganisms could be introduced during manufacture, we also carried out the British Pharmacopoeial 2012 (*BP*) test for Preservative Efficacy (*BP*, 2012). *S. aureus* and *P. aeruginosa* suspensions were prepared to give a final inoculum of 10^8 colony-forming units/ml (cfu/ml). The *C. albicans* suspension was prepared to give a final inoculum of 10^7cfu/ml and *A. brasiliensis* came as a 5.8×10^7cfu/ml suspension. According

to the BP, the preparation should be challenged with an inoculum between 10^5 to 10^6 cfu/g/ml of bacteria and fungi and tested over 28 days. Therefore, 10 μl of the microorganism suspensions were added to separate 1.5 ml eppendorfs with 1.0 g of the MN gel formulations. The MN were then prepared as described above and then added to vials containing 10 ml of PBS pH 7.4. In accordance with the BP test for preservation for preparations for cutaneous application, total viable counts were completed on the MN after 2, 7, 14 and 28 days using standard plate counting methods. Testing of the aqueous gel used to prepare the MN gave a result for day 0.

Radiolabelling of microorganisms

One colony of each of *C. albicans*, *P. aeruginosa* and *S. aureus* was inoculated into 25 ml of MHB containing 100 μl of [^{3}H] thymidine (1.0 mCi ml^{-1}) and incubated for 18 h at 37°C, as described previously (Donnelly *et al*., 2009b). Briefly, the suspension was centrifuged (3000 rpm, 10 min), washed twice in cold PBS and resuspended to an optical density at 550 nm equivalent to 1.0×10^7 cfu ml^{-1}. To determine the relationship between disintegrations per minute (dpm) and viable count, 1.0 ml aliquots of each labelled suspension were added separately to vials containing 5.0 ml of liquid scintillation cocktail (Ultima gold™, PerkinElmer, Boston, USA).Vials were stored in darkness for 2.0 h prior to analysis to reduce chemiluminescence to less than 1% in respect of the total count. Samples were then counted in a scintillation counter (Tricarb 1900 TR, LS Analyzer, Packard, USA) for 30 min. Conversion to dpm was achieved against quench correction curves. Mean dpm values from three replicate experiments were then related to the total viable count of microorganisms present.

Permeation of radiolabelled microorganisms across porcine skin

Neonate porcine skin, a good model for human skin (Fourtanier and Berrebi, 1989; Woolfson *et al*., 1995), was obtained from stillborn piglets and immediately (<24 hours after birth) excised, trimmed to a thickness of 400 μm using a dermatome (Integra Life Sciences™, Padgett Instruments, NJ, USA) and frozen in liquid nitrogen vapour, as previously described (Donnelly *et al*., 2009b; Donnelly *et al.*, 2010; Donnelly *et al*., 2011; Donnelly *et al*., 2012b). Skin was then stored in aluminium foil at -20°C for no more than 7 days prior to use. The porcine skin was then sandwiched between the receptor and donor compartments of the modified Franz cells using sterile forceps.

An identical set-up to that previously employed for silicon MN was used (Donnelly *et al*., 2009b). Briefly, an aliquot (1.0 ml) of microbial suspension containing 1×10^7 cfu ml^{-1} was placed in the donor compartments of the Franz-cells and left in place for 24 h. Donor compartments were covered with sterilised lids to prevent buffer evaporation and avoid contamination. After 24 h, suspensions containing microorganisms not adhered to the skin were removed from the donor compartments and the skins were either not punctured (Control) or punctured (Test) in one of three different ways, namely; (i) Punctured with MN which were left in place for 24 h, (ii) Punctured with MN which were removed and (iii) Punctured with a hypodermic needle (21G) which was removed. Control experiments were also run in a similar fashion, but without puncturing the membranes. A poly (vinyl chloride) (PVC) probe with MN attached to the base and an aluminium slab attached at the top was

used for skin puncture, which was done with gentle hand pressure by a researcher experienced in MN application. Where MN were left in place after puncture, the skin was punctured with the help of stainless steel clamps that pressed the PVC probe assembly against the skin, creating holes on the surface. The entire assembly was then left in place for 24 h. When MN were removed after puncture, the probe assembly was removed within 30 sec after application. When a 21G sterile hypodermic needle (21G × 1 ½", Terumo Neolus, Leuven, Belgium) was used, the skin was punctured slowly by hand, with the full length of the needle inserted and then removed within 30 sec. A digital microscope (GXMGE-5 USB Digital Microscope, Laboratory Analysis Ltd, Devon, UK) was used to confirm the presence of holes in the skins in preliminary studies. Twenty four hours after puncture, the Franz cells were dismantled. Skin samples were then placed on an aluminium stub and covered with an aluminium ring, exposing only the diffusional area of 15 mm^2. The skin was then subjected to tape-stripping to remove the *stratum corneum* (Moser *et al*., 2001, Pellett *et al*., 1997). The skin was dabbed dry with the first tape strip (15 × 18 mm) and this and the following 12 ± 3 tape strips were placed in a scintillation vial. To ensure intimate contact between the tape and skin, forceps were used to apply gentle pressure for each tape strip. Complete removal of the *stratum corneum* was indicated by the glistening of the viable epidermal layer after removal of the final tape strip (Pellett *et al*., 1997). An aliquot (5.0 ml) of dimethyl sulfoxide was then added to the vial to dissolve the tape and *stratum corneum*. The viable tissue remaining was dissolved in 1.0 ml of tissue solubilizer (NCS® -II, Amersham Biosciences, England, UK) in a scintillation vial. Both sample types were then incubated at 60°C for 12 h. Liquid samples (1.0 ml) of the tape-stripped *stratum corneum*, viable tissue and the receptor solution removed at the end of the experiment were then added separately to vials containing 5.0 ml of liquid scintillation cocktail, which were again stored in darkness for 2.0 h prior to analysis. Samples were then counted in the scintillation counter for 30 min. Mean dpm values from three replicate experiments were converted to total viable count of microorganisms present.

Since it could be argued that it may be possible for microorganisms present in the transdermal patch could move across the hydrogel matrix of the MN and into viable skin, a separate experiment was conducted. The set-up was as described above, except that the sidewalls were not removed from the MN after de-moulding. Instead, these sidewalls were allowed to form an open box, with a wall height of approximately 5.0 mm. MN were then inserted into skin and into this "container" was separately placed 1.0 ml aliquiots of each of the radiolabelled microorganisms described above, again at 1×10^7 cfu ml^{-1} (Figure 4). At the end of the 24 hour experiment, skin and receiver compartment fluid was treated as above to assay for the presence of radiolabelled microorganisms.

Clinical studies in human volunteers

Hydrogel-forming MN (height of 280 μm, a diameter of 240 μm at the base, and an interspacing of 750 μm between rows of MNs with 7×7 arrays) were applied using gentle thumb pressure to the ventral forearm skin of six non-smoking healthy volunteers (3 men and 3 women) aged between 23 and 31 years, with no pre-existing skin conditions. Waterproof plasters (Elastoplast® , Hamburg, Germany) were used to keep MN in place for 24 hours. Controls included removing the MN-plaster immediately upon application,

applying only MN baseplates for 0 h and 24 h and applying only the plasters for 0 h and 24 h. Parameters such as pain, trans-epidermal water loss (TEWL) and clinical skin appearance were determined independently by two Consultant Dermatologists (NMcL & KA) blinded to the skin treatments performed. Volunteers were followed up for 4 weeks for evidence of local or systemic infection.

Statistical Analysis

Where appropriate, statistical analyses of the results were performed with a one-way analysis of variance (ANOVA), where $p < 0.05$ was taken to represent a statistically significant difference. When there was a statistically significant difference, post-hoc Tukey's HSD multiple comparison test was then performed. Microbial data was analysed using the Mann-Whitney U-test. Statistical Package for the Social Sciences, SPSS 17.0 version 2.0 (SPSS, Inc., Chicago, IL), was used for all analyses.

Results

Figure 5A shows a decrease in the height of MN with increase in the axial forces applied. The reduction in MN height was approximately linear with increase in the forces applied. For example, at a force of 0.20 N per needle, the decrease in MN height was 0.202 ± 0.06 mm. Figure 5B shows digital microscope images of the MN after subjecting them to axial forces. Skin penetration of the MN was investigated using dermatomed neonatal porcine skin and the percentage number of holes (micro-conduits) created by the MN arrays was determined after staining with methylene blue solution, as described previously (Donnelly *et al*., 2009a; Migalska *et al*., 2011). In general, increasing the forces applied per MN array increased the penetration efficiency of the MNs, as shown in Figure 6. The micro-conduits created by the MN array are much more clearly visible at higher applied forces compared to the lower forces. For example, the percentage numbers of micro-conduits, created after penetration tests, were ≈ 70%, 90% and 100% at insertion forces of 0.05 N, 0.20 N and 0.40 N per needle, respectively. Micro-conduits could also be traced on the surface of the laboratory film (Parafilm®) (Figure 6) underneath the skin, which indicates that, at higher insertion forces, the depth of penetration was higher. Microscope images of the MN following removal from the skin did not show any damage to the hydrogel MN structure, regardless of applied force, although some swelling at the tips was observed (Figure 6).

Forces required to break the hydrogel-based MN base-plates and the angle of bending of the MN base-plates before breaking are presented in Figure 7. The average angle of bending of MN base-plates was 79.28°, indicating a good degree of flexibility of the hydrogel-forming MN base-plates. Figure 8 shows images following transverse failure forces tests, required to break the MN arrays, using a novel Texture Analyser set-up described previously (Donnelly *et al*., 2011). The probe was moved perpendicularly towards the MN and transverse failure force was determined by breaking away the MN from their base-plate (therefore causing a 100% reduction in MN height). The mean force required to break (100% reduction of MN height) the MNs was 0.56 N per needle. However, the forces required to break at 60% of MN height were significantly lower than break strength at 100% ($p < 0.001$, in each case).

After subjecting to short-term stability studies, MN base-plates and MN arrays were analysed for different parameters. Firstly, the folding endurance of the MN base-plates was determined, as shown in Table 1. It was observed that the FE of all three different types of MN base- plates remained zero before subjecting to stability studies and after storing at 0% RH and 43% RH for 21 days. However, FE of MN base-plates when stored at 86% RH was greater than zero, indicating that the MN base-plates become soft/rubbery in nature. The change from a hard/glassy to soft/rubbery state of the MN base-plates was further tested by determining the glass-transition temperature (T_g) of the samples using DSC. Figure 9A shows the change in the T_g of the MN base-plates over time during the stability studies. The T_g values of MN base-plates before subjecting to stability studies were 55.82 ± 0.97 °C. When stored at 0% RH, MN base-plates, did not show any significant changes in the T_g. In contrast, a significant drop in T_g values was observed when MN base-plates were stored at 43% and 86% RH, respectively. The percentage of residual water content of the MN base-plates before subjecting to stability studies was 2.96 ± 0.35. Figure 9B shows the water content of the MN base-plates analysed at different intervals and RHs. No statistically significant difference in water content was observed for MN base-plates stored at 0% RH. In contrast, MN base-plates, when stored at 43% and 86% RH, showed significant increases in water content. The increase in the % water content of MN base-plates also caused increases in the weight of MN base-plates. Stability studies revealed that the MN arrays, prepared from the hydrogel-forming material when stored at 0% RH and 43% RH, preserved their mechanical strength (i.e., fracture force under axial load) during storage, as determined by fracture force tests. Based on the percentage reduction in height, following fracture force analysis (Figure 10A), the mechanical strength of the MN arrays was found to be the same after storing for 14 days at an RH of 0 and 43%. There was no statistically significant change in the reduction of MN height. However, MN stored at 86% RH absorbed so much moisture (as shown in Figure 10B), that all MN became deformed. Accurate measurement of MN height and subsequent fracture force analysis was, therefore, impossible. Importantly, no microbial growth was evident in any of the MN arrays, with no exceptions to this among the different storage times and conditions.

The microbiological examination, conducted according to *Ph Eur* test 2.6.12, of non-sterile aqueous hydrogels and the crosslinked hydrogel MNs indicated no growth of colony-forming units (CFU) of microorganisms. According to the *Ph Eur*, the acceptance criteria for transdermal patches are 10^2 CFU/g or CFU/ml for total aerobic microbial count and 10^1 CFU/g or CFU/ml for total yeast microbial count. However, the acceptance criteria for parenteral injection are complete sterility (ie no contaminating microorganisms). The number of CFU per aqueous hydrogel or crosslinked MN array in the stock solution, in MHA and SDA plates, was zero. The experiment was repeated with more concentrated stock solutions. However, the number of CFU still remained zero, which indicates the absence of viable microorganisms in aqueous gels as well as crosslinked MN arrays. Tests for specific microorganisms (*E. coli*, *S. aureus*, *P. aeruginosa*, *C. albicans* and *A. brasiliensis*) also showed no growth. The *BP* Test for Preservative Efficacy (Table 2) was passed by the hydrogel-forming MN formulation for all microorganisms, indicating that the microorganisms deliberately added did not survive the process of MN fabrication and

crosslinking (Table 3). This was despite each of the microorganisms added initially being detectable in the gels used to prepare the microneedles.

As in our previous studies (Donnelly *et al*., 2009b), *P. aeruginosa* did not take up enough radiolabelled thymidine to allow reliable results to be obtained. Studies with *C. albicans* and *S. epidermidis* showed that the majority of the microbial load initially attached to the *stratum corneum* remained attached and did not penetrate the skin, regardless of puncture protocol (Table 4). For both *C. albicans* and *S. epidermidis*, approximately 10^4 cfu moved into viable skin following puncture with the hypodermic needle, but in each cases less than 1% of the total number attached to control *stratum corneum* entered viable epidermal skin. Permeation of *C. albicans* and *S. epidermidis* into viable epidermal skin was actually higher for the MN groups, being of the order of 10^5, regardless of MN puncture protocol. These results showed a similar trend as that we observed using silicon MN of similar dimensions (Donnelly *et al*., 2009b). Importantly, no microorganisms were detectable beyond the epidermal skin in the receptor fluid when MN were used to puncture the skin. This was in contrast to the data obtained using the hypodermic needle, where approximately 10^6 microorganisms were detected in the receptor fluid for both *C. albicans* and *S. epidermidis*. The number of invading microorganisms required to cause an infection has been estimated as 10^4 (Seal *et al*., 2000), but ultimately depends on pathogen and host response factors. We have shown here that, with a microbial load of approximately 1×10^7 cfu cm^{-2} on the *stratum corneum*, hypodermic needle puncture allowed more than 10^4 microorganisms to penetrate into the viable tissue and 10^6 cfu of *C. albicans* and *S. epidermidis* to completely cross the epidermal skin in 24 h following needle puncture. However, in the developed World, appropriate use of hypodermic syringes does not routinely cause infection (WHO, 2012), despite the facts that bacteria are found as part of the normal skin flora in numbers ranging from 10^2–10^6 cfu cm^{-2} depending on location and that alcohol decontamination of skin prior to injection is not completely effective (Del Mar *et al*., 2001; Pittet *et al*., 2006). This suggests that bacterial numbers entering skin following hypodermic needle puncture are not sufficient to cause infection in normal circumstances. This is probably due to the fact that skin has a number of highly effective innate defence mechanisms such as lowered pH (pH 5-6), inhibitory lipids and antimicrobial peptides (Elsner *et al*., 2006) and is a major immune-competent organ replete with professional antigen-presenting cells (Al-Zahrani *et al*., 2012).. Routine needle-based administration of therapeutics is not typically associated with severe or irritating local skin reactions. Accordingly, it would not be expected that the immune cells in skin would initiate or potentiate any noticeable local side effects in the course of their activities in dealing with microorganisms entering the viable skin due to MN application. Notably, no microorganisms were detectable in the hydrogel penetration study, either in the skin or in the receiver compartment fluid, indicating, unsurprisingly, that these microorganisms were unable to permeate through the swelling MN matrices.

In the clinical study involving 6 volunteers, visual analogue scale (VAS) scores of pain were measured for the three patches, immediately after patch application and upon patch removal, as shown in Figure 11. No statistically significant difference was observed between the VAS scores measured following application of the patches (comprised hydrogel MNs arrays, MN base-plates and patch only) on the two different treatments (i.e. 0 & 24 hrs) studied. For

example, the mean VAS score for application of patch only was 0.92 cm, which was not significantly different from that for patches applied containing either MN arrays (0.84 cm, $p = 0.754$) or MN base-plate (0.87 cm, $p = 0.203$), in a 24 hrs treatment (Figure 11). Similar results were observed for 0 hr treatment. In addition, VAS scores were also measured during patch removal, as presented in Figure 11B. No statistically significant difference was observed between the VAS scores following removal of patches at the three different treatments (i.e., 0 & 24 hrs) studied. For example, the mean VAS score after removing the patch only was 0.45 cm, which was not significantly different from patches containing MN arrays (0.48, $p = 0.120$) or MN base-plates (0.31cm, $p = 0.695$) in a 24 hrs treatment.

TEWL measurements were taken from each volunteer before and after patch application and at all the three different treatments (i.e., 0 & 24 hrs) studied. During each measurement, the volunteer was rested for at least 15 min. Figure 12 shows the results of TEWL values determined during the three different treatments. Prior to treatment, mean TEWL values were 10.95 g h^{-1} m^{-2}. Following the 0 hr treatment, no significant increase in TEWL values was observed compared to baseline value in each case (Figure 12), but at 30 min after patch removal, the TEWL values decreased and reached values that were below the baseline values in each case.

After 24 hr of treatment with all the three patches (i.e. comprised of hydrogel MNs arrays, MN base-plates and patch only) a significant increase in TEWL values was observed immediately and declined after 15 min reaching baseline values after 30 min, as shown in Figure 12. For example, when patches only were removed after 24 hrs TEWL values increased significantly ($p = 0.014$) and immediately to 56.62 g h^{-1} m^{-2} of its baseline value of 9.67 g h^{-1} m^{-2}. However, in this case, a huge standard deviation of 61.55 g h^{-1} m^{-2} was observed. This was because one of the volunteers showed a TEWL value of 175 g h^{-1} m^{-2}. Patches containing MN base-plate when removed after 24 hrs the TEWL values showed significant ($p < 0.05$) increase immediately to 24.80 g h^{-1} m^{-2} of the baseline value of 10.57 g h^{-1} m^{-2}. Similarly, when patches containing MN arrays were removed after 24 hrs, the TEWL values increased significantly ($p < 0.05$) and immediately to 34.40 g h^{-1} m^{-2} of the baseline value of 10.70 g h^{-1} m^{-2}. However, the order of increase in the TEWL values immediately after patch removal was highest for patch only (56.62 g h^{-1} m^{-2}), followed by patch containing MN arrays (34.40 g h^{-1} m^{-2}) and patch containing MN base-plate (24.80 g h^{-1} m^{-2}), respectively.

The clinical photographs collected from each treatment protocol were scored by visual inspection and an Irritant Contact Dermatitis (ICD) score was assigned to each photograph (Astner *et al.*, 2006). Figure 13 shows some sample clinical photographs taken before and after removal of the patches following 24 hrs treatments. Table 5 shows the ICD scores of the individual volunteers for the two different treatments. It can be observed from the clinical scores that the patch only had minimal score ranging from 0 to 1, patch containing MN base-plate showed scores ranging from 0 to 2 and patch containing MN arrays showed scores ranging from 0 to 3. However, in all cases, ICD scores were found to be 0 within 1 hr of removal of the MN arrays, indicating complete absence of erythema. In addition, the MN arrays remained intact and that no damage or loss of the MNs was noted during the application, during wear, regardless of how long they were in place, or while removing them

from the ventral forearm of volunteers. OCT investigations showed swelling of these MNs. For example the 280 μm height hydrogel MNs penetrated to a depth of 190 ± 12 μm with pore width of 97 ± 12 μm, which changed to dimensions of 243 ± 22 μm in depth and 137 ± 11 μm in pore diameter flowing *in vivo* swelling, as represented in Figure 14.

Discussion

Despite having a mechanism of action that necessitates breaching the protective barrier of the skin, the *stratum corneum*, microneedle application has never been associated with skin or systemic infection in the numerous clinical trials carried out involving many thousands of patients (Donnelly *et al*., 2012a). However, these studies all employed metal or silicon microneedles that can be easily rendered sterile by gamma irradiation or aseptic manufacture. Microneedle arrays prepared from aqueous polymer gels present many advantages over their first generation counterparts, in that they can be loaded with drug substance, rather than simply coated, allowing greater doses to be delivered and enhanced control over rate of drug release. Hydrogel-forming microneedles provide for even greater dosing capacity and control. Importantly, however, such systems present a unique set of challenges, due to the propensity for microbial growth in aqueous environments. Aseptic processing can be complex when the excipients used for microneedle fabrication are received in a non-sterile state. In addition, the facilities necessary are expensive to maintain. Terminal sterilisation by gamma irradiation can potentially could possibly unwanted polymer crosslinking (Dawes *et al*., 1996) and possible drug degradation in dissolving systems (Seo *et al*., 2007).

The hydrogel-forming microneedle arrays described here appear to possess in-built antimicrobial properties, with no viable microorganisms present in the content tests and none capable of surviving the micromoulding and crosslinking steps in the preservation test. No microbial growth was evident during storage, regardless of conditions. These observations are hardly surprising, given the low pH of the gel (pH 2), the temperature required for crosslinking (24 h at 80°C) and the apparent inherent antimicrobial properties of the polymer (Boehm *et al*., 2012). It is important to note, however, that crosslinking renders the formed microneedles neutral, such that no pH change is evident when swollen in non-buffered water (pH 6.5). Indeed, no detrimental effects were observed in 2D and 3D cell cultures exposed to aqueous extracts of this microneedle material (Donnelly *et al*., 2012b). No detectable microbial penetration occurred through the swelling MN, possibly to do with the highly hydrophilic nature of the hydrogel material and the relatively large size of microbial cells compared to drug substances. The human volunteer studies carried out here also showed no adverse effects and no evidence of infection upon follow-up. Indeed, microbial penetration through microneedle-induced holes into viable skin *in vitro* was found to be minimal, despite the exaggerated microbial loadings used on the *stratum corneum* surfaces.

Conclusions

The findings presented here indicate that progressing towards commercial exploitation and clinical application with microneedle arrays prepared from aqueous polymeric gels may not

prove as problematic as one may assume. Indeed, the hydrogel-forming microneedles investigated here have notable advantages over other polymeric systems due to the nature of the formulation and the heating step required for crosslinking. With such a system, it does not appear it will be necessary to prepare the microneedles aseptically, include an antimicrobial preservative or employ terminal gamma sterilisation in order to protect patient safety. While microbial levels in the attached transdermal patches will be necessarily low to comply with pharmacopoeial standards it does not appear that microbial permeation through the swelling microneedles into viable skin will be possible, thus removing another potential concern. Since no pharmacopoeial standards currently exist for microneedle-based products, the exact requirements for a proprietary product based on hydrogel-forming microneedles are at present unclear. However, we are currently working with a number of commercial partners towards a comprehensive specification set for this microneedle system that may inform future developments in this regard.

Acknowledgments

This study was supported by BBSRC grant numbers BB/FOF/287 and BB/E020534/1 and Wellcome Trust grant number WT094085MA.

References

Al-Zahrani S, Zaric M, McCrudden C, Scott C, Kissenpfennig A, Donnelly RF. Microneedle-mediated vaccine delivery: Harnessing cutaneous immunobiology to improve efficacy. Exp.Opin. Drug Deliv. 2012; 9:541–550.

Astner S, Burnett N, Rius-Díaz F, Doukas AG, González S, Gonzalez E. Irritant contact dermatitis induced by a common household irritant: a noninvasive evaluation of ethnic variability in skin response. J. Am. Acad. Dermato.l. 2006; 54:458–465.

BBC Weather report. Online 2008 Febrauray. Available from URL:http://www.bbc.co.uk/weather/world/city_guides/results.shtml?tt=TT003790

British Pharmacopoeia. Appendix XVI C. Efficacy of antimicrobial preservatives in pharmaceutical products. 2012; Vol. V:A454–A456.

Boehm RD, Miller PR, Singh R, Shah A, Stafslien S, Daniels J, et al. Indirect rapid prototyping of antibacterial acid anhydride copolymer microneedles. Biofabrication. 2012 doi: 10.1088/1758-5082/4/1/011002.

Dawes, K.; Glover, LC. Physical Properties of Polymers Handbook. Mark, James E., editor. American Institute of Physics Press; Woodbury, NY: 1996.

Del Mar CB, Glasziou PP, Spinks AB, Sanders SL. Is isopropyl alcohol swabbing before injection really necessary? Med. J. Aust. 2001; 174:306. [PubMed: 11297122]

Donnelly RF, Morrow DIJ, Singh TRR, Migalska K, McCarron PA, O'Mahony C, et al. Processing difficulties and instability of carbohydrate microneedle arrays. Drug Dev. Ind. Pharm. 2009a; 35:1242–1254. [PubMed: 19555249]

Donnelly RF, Singh TRR, Tunney MM, Morrow DIJ, McCarron PA, O'Mahony C, et al. Microneedle arrays allow lower microbial penetration than hypodermic needles *in vitro*. Pharm. Res. 2009b; 26:2513–2522. [PubMed: 19756972]

Donnelly RF, Garland MJ, Morrow DIJ, Migalska K, Thakur RRS, Majithiya R, Woolfson AD. Optical coherence tomography is a valuable tool in the study of the effects of microneedle geometry on skin penetration characteristics and in-skin dissolution. J. Cont. Rel. 2010; 147:333–341.

Donnelly RF, Majithiya R, Singh TRR, Morrow DIJ, Garland MJ, Demir Y, et al. Design and physicochemical characterisation of optimised polymeric microneedle arrays prepared by a novel laser-based micromoulding technique. Pharm. Res. 2011; 28:41–57. [PubMed: 20490627]

Donnelly, RF.; Singh, TRR.; Morrow, DIJ.; Woolfson, AD. Microneedle-mediated Transdermal and Intradermal Drug Delivery. Wiley Online Library; 2012a.

Donnelly RF, Singh TRR, Garland MJ, Migalska K, Majithiya R, McCrudden CM, et al. Hydrogel-Forming Microneedle Arrays for Enhanced Transdermal Drug Delivery. Adv. Funct.l Mat. 2012b; 22:4879–4890.

Elsner P. Antimicrobials and the skin physiological and pathological flora. Current Problems in Dermatology, Basel. 2006; 33:35. (R).

European Pharmacopoeia 6.5. Methods of analysis; 2.6.12 Microbiological examination of non-sterile products: Microbial Enumeration Tests. European Pharmacopoeia 6.5. 2007:4769–4773.

Fourtanier A, Berrebi C. Miniature pig as an animal model to study photoaging. Photochem. Photobiol. 1989; 50:771–784. [PubMed: 2626491]

Global Biotechnology Market to Surpass US$320 Billion by 2015, According to New Report by Global Industry Analysts. 2012. Online. Available from URL: www.prweb.com/releases/biotechnology/biotech_services_crops/prweb9128590.htm

Greystone Associates. Microneedles in Medicine: Technology, Devices, Markets and Prospects. Greystone Associates; Amherst, NH: 2012.

Migalska K, Morrow DIJ, Garland MJ, Thakur RRS, Woolfson AD, Donnelly RF. Laser-engineered dissolving microneedle arrays for transdermal macromolecular drug delivery. Pharm. Res. 2011; 28:1919–1930. [PubMed: 21437789]

Moser K, Kriwet K, Froehlich C, Kalia YN, Guy RH. Supersaturation: enhancement of skin penetration and permeation of a lipophilic drug. Pharm. Res. 2011; 18:1006–1011. [PubMed: 11496937]

Pellett M, Roberts M, Hadgraft J. Supersaturated solutions evaluated with an in vitro stratum corneum tape stripping technique. Int. J. Pharm. 1997; 151:91–98.

Pittet D, Allegranzi B, Sax H, Dharan S, Pessoa-Silva CL, Donaldson L, et al. Evidence-based model for hand transmission during patient care and the role of improved practices. The Lancet Infectious Diseases. 2006; 6:641–652. [PubMed: 17008173]

Pharmaceutical and Medical Packaging News (PMPN) Magazine. Oct. 2012 Online. Available from URL: http://www.pmpnews.com/pmpn-indexad.html?gotourl=http://www.pmpnews.com/news/transdermal-delivery-market-predictedreach-315-billion-2015-pharmalive-special-report

Seal, DV.; Hay, RJ.; Middleton, KR. Skin and Wound Infection: Investigation and Treatment in Practice. Informa Healthcare.: Martin Dunitz; London: 2000. p. 5-8.

Seo J, Kim J, Lee J, Yoo Y, Kim MR, Park K, et al. Ovalbumin modified by gamma irradiation alters its immunological functions and allergic responses. Int. Immunopharmacol. 2007; 7:464–472. [PubMed: 17321469]

Ubaidulla U, Reddy MVS, Ruckmani K, Ahmad FJ, Khar RK. Transdermal therapeutic system of carvedilol: Effect of hydrophilic and hydrophobic matrix on in vitro and in vivo characteristics. AAPS PharmSciTech. 2007; 8:13–20. [PubMed: 17408213]

Woolfson AD, McCafferty DF, McCallion CR, McAdams E, Anderson J. Moisture-activated, electrically conducting bioadhesive hydrogels as interfaces for bioelectrodes: Effect of film hydration on cutaneous adherence in wet environments. J. Appl. Polym. Sci. 1995; 58:1291–1296.

World Health Organization. Nov. 2012 Online. Available from URL: www.who.int/en

Europe PMC Funders Author Manuscripts

Highlights

- We describe, for the first time, the microbial characterisation of hydrogel-forming polymeric microneedle arrays and the potential for passage of microorganisms into skin following microneedle penetration
- Microneedle materials did not support microbial growth
- The numbers of microorganisms crossing the *stratum corneum* following microneedle puncture was greater than 10^5 cfu in each case. However, no microorganisms crossed the epidermal skin
- When using a 21G hypodermic needle, more than 10^4 microorganisms penetrated into the viable tissue and 10^6 cfu of *C. albicans* and *S. epidermidis* completely crossed the epidermal skin in 24 h
- Human volunteer studies confirmed that skin or systemic infection is highly unlikely when polymeric microneedles are used for transdermal drug delivery.

Europe PMC Funders Author Manuscripts

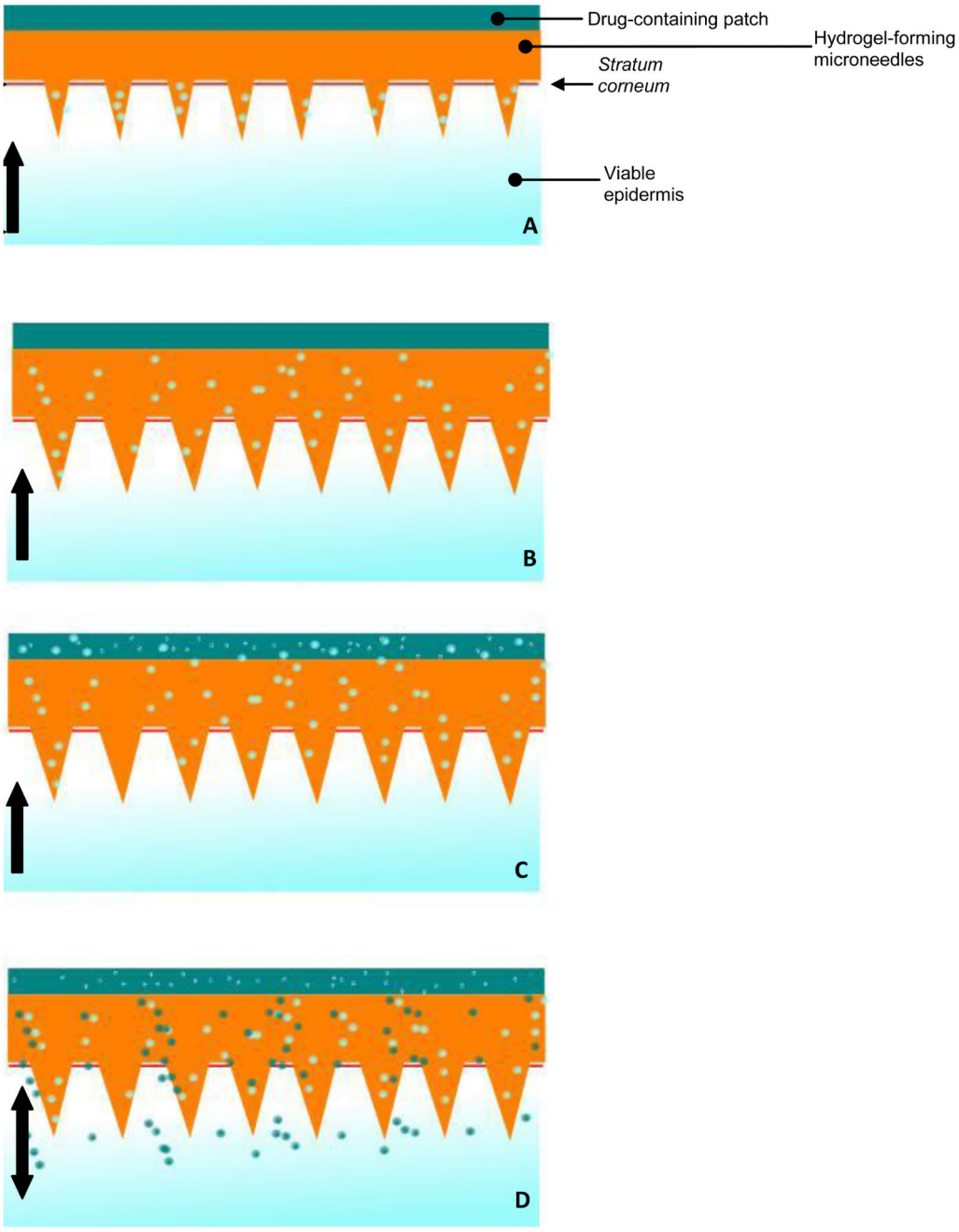

Figure 1.

Illustration of phenomena involved in the swelling and subsequent permeation of drug substances from the novel PEG-PMVE/MA-based hydrogel MN arrays. Skin insertion (A), followed by rapid uptake of skin interstitial fluid (B), liberation of drug from the patch (C) and subsequent drug diffusion into the viable epidermis (D).

Europe PMC Funders Author Manuscripts

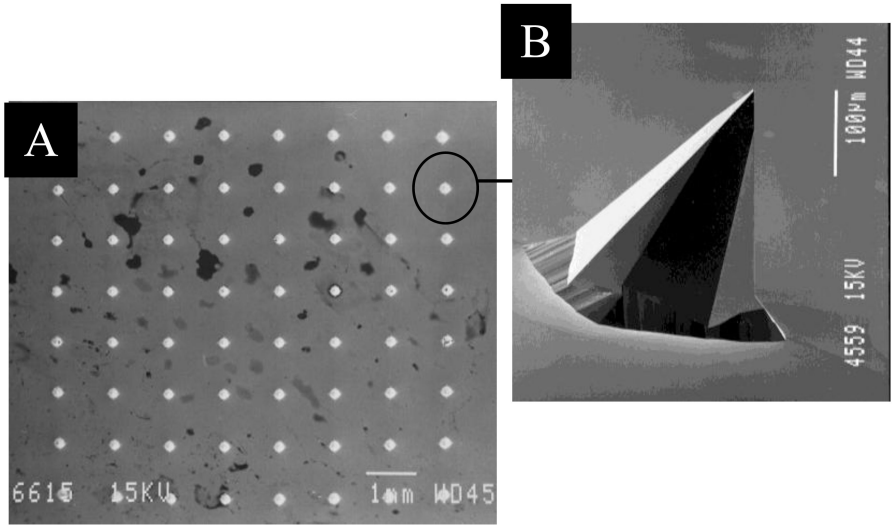

Figure 2.
SEM images taken of a typical silicon microneedle array from (A) directly above and of (B) a lateral view of single microneedle.

Europe PMC Funders Author Manuscripts

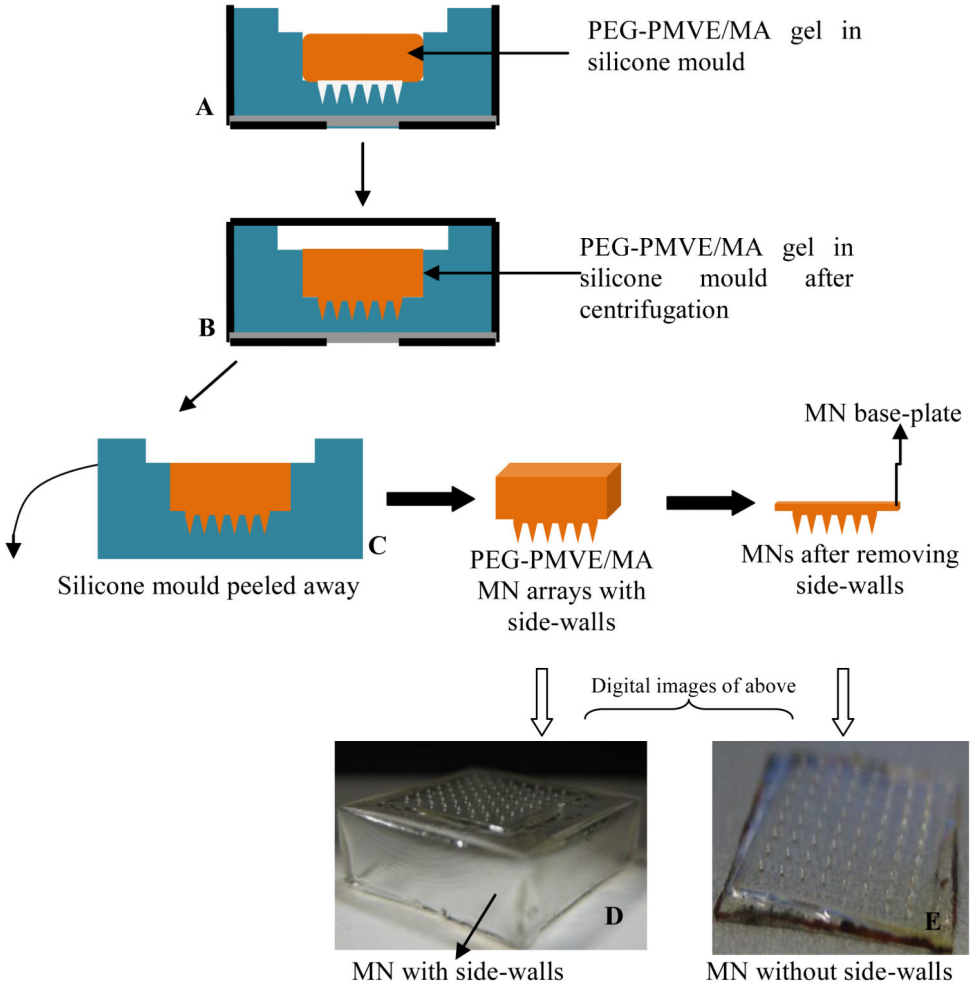

Figure 3.

Diagrammatic representation of the steps involved in the preparation of PEG-crosslinked PMVE/MA microneedles. PEG-PMVE/MA gel is transferred to the silicone mould (A). The mould is centrifuged at 3500 rpm for 15 minutes (B). Crosslinking is performed at 80°C for 24 hours and the silicone mould is carefully peeled away to form PEG-corsslinked PMVE/MA MN arrays (C). Digital photograph image of microneedles with side-walls (D). Digital image of MN after cutting away the side-walls using a hot scalpel blade (E).

Europe PMC Funders Author Manuscripts

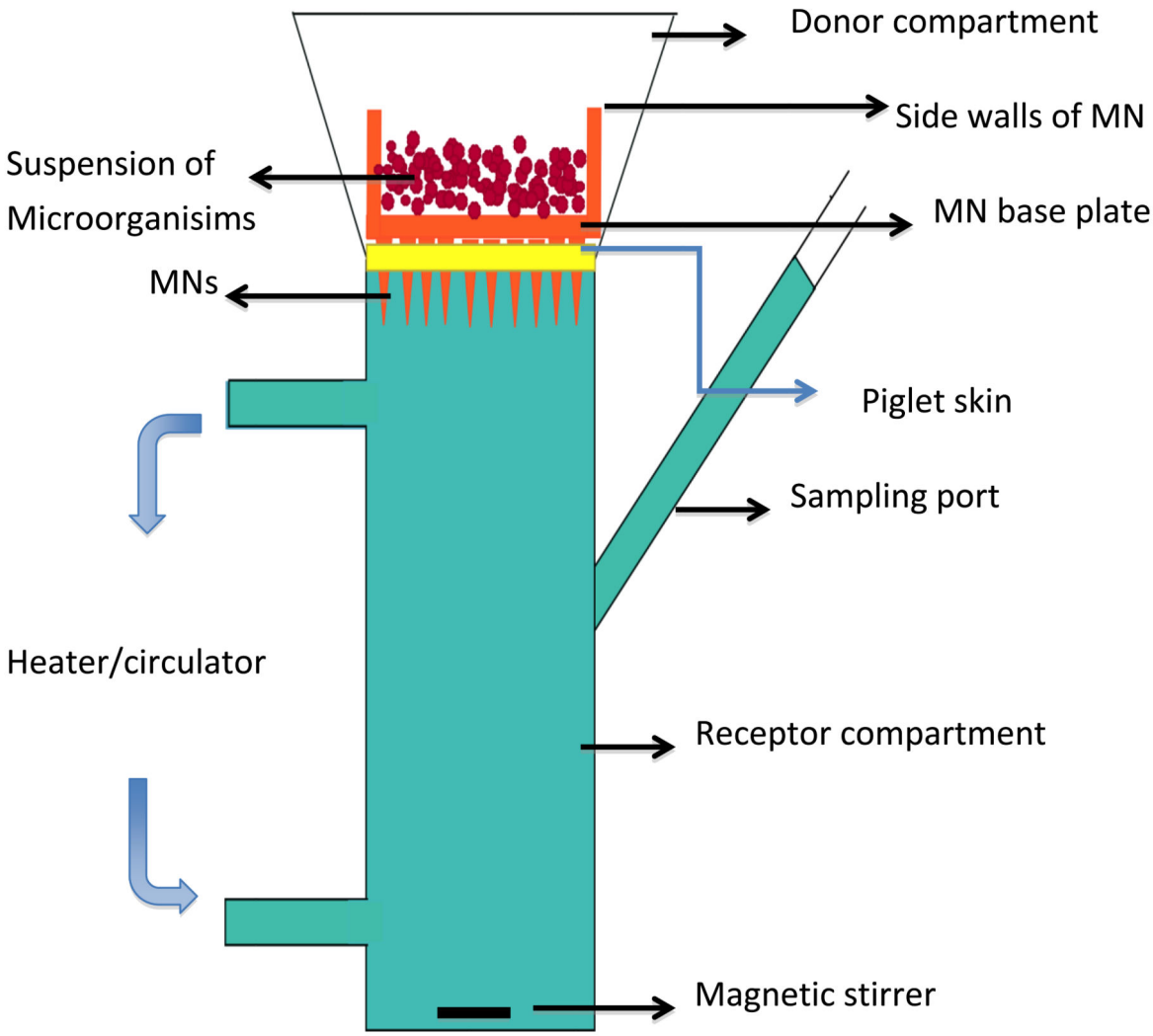

Figure 4.
Experimental set up used to investigate microbial penetration through hydrogel-forming microneedle arrays.

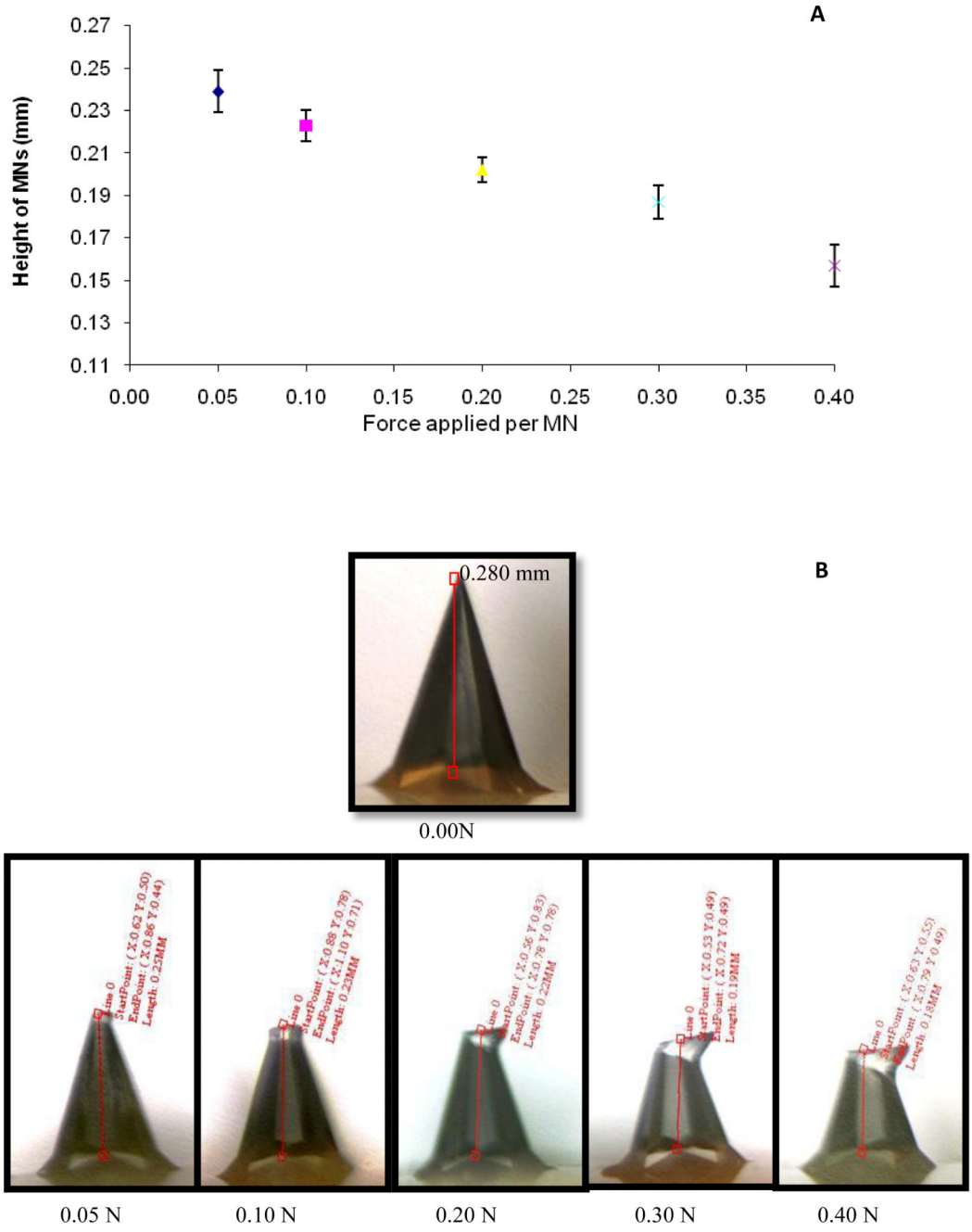

Figure 5.

Decrease in the height of microneedles following application of axial loads. Means ± S.D. N = 6 (A) and digital images representing a decrease in the height of F2 MNs, after subjecting them to fracture force by axial load (B).

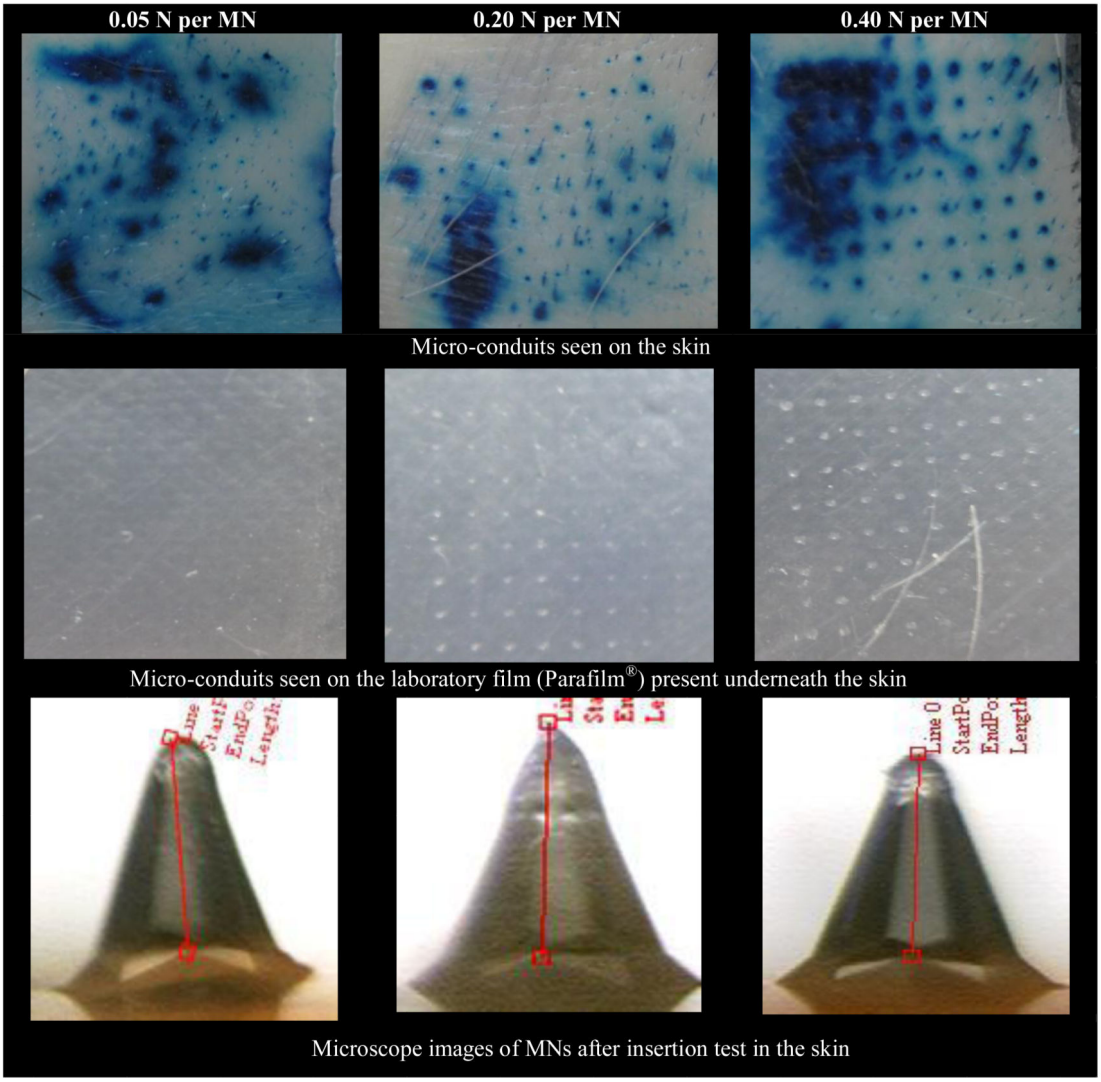

Figure 6.

Digital images showing micro-conduits on skin and their respective images on laboratory film (Parafilm®) created following insertion of F2 hydrogel MNs, at different forces.

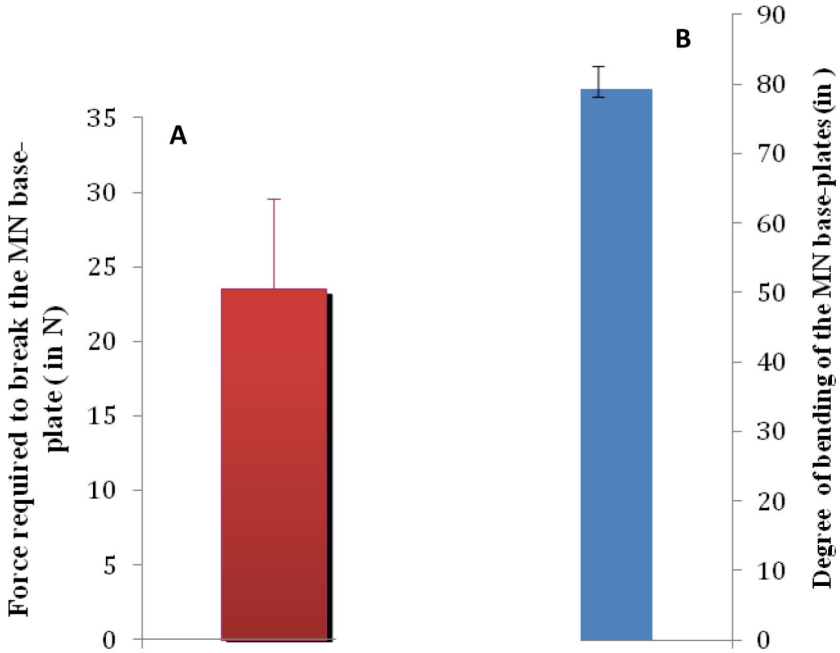

Figure 7.
Break strength (A) and angle of bending (B) of the microneedle base-plates.

Europe PMC Funders Author Manuscripts

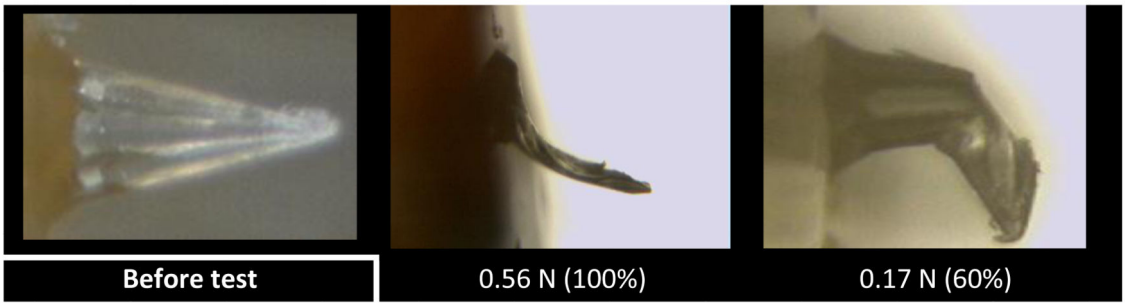

Figure 8.
Digital microscope images of microneedles before and after transverse failure force tests determined by breaking the respective MNs at 100% and 60% of MN height from their base-plate.

Europe PMC Funders Author Manuscripts

Europe PMC Funders Author Manuscripts

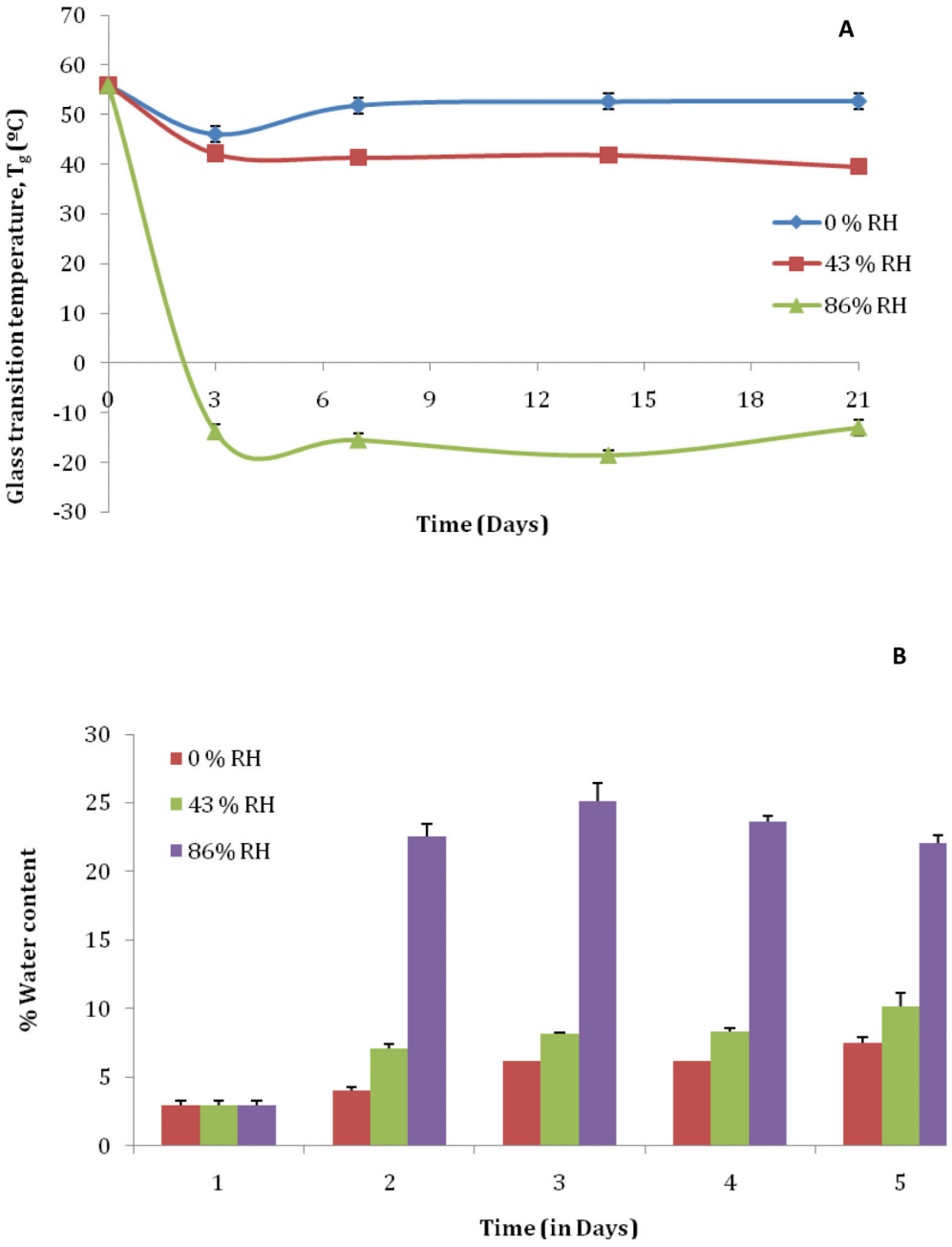

Figure 9.

Change in T_g of F2 MN base-plates following sampling at different time intervals during stability studies (means ± SD, N = 3) (A) and water content of F2 MN base-plates following sampling at different time intervals during stability studies (means ± SD, N = 3) (B).

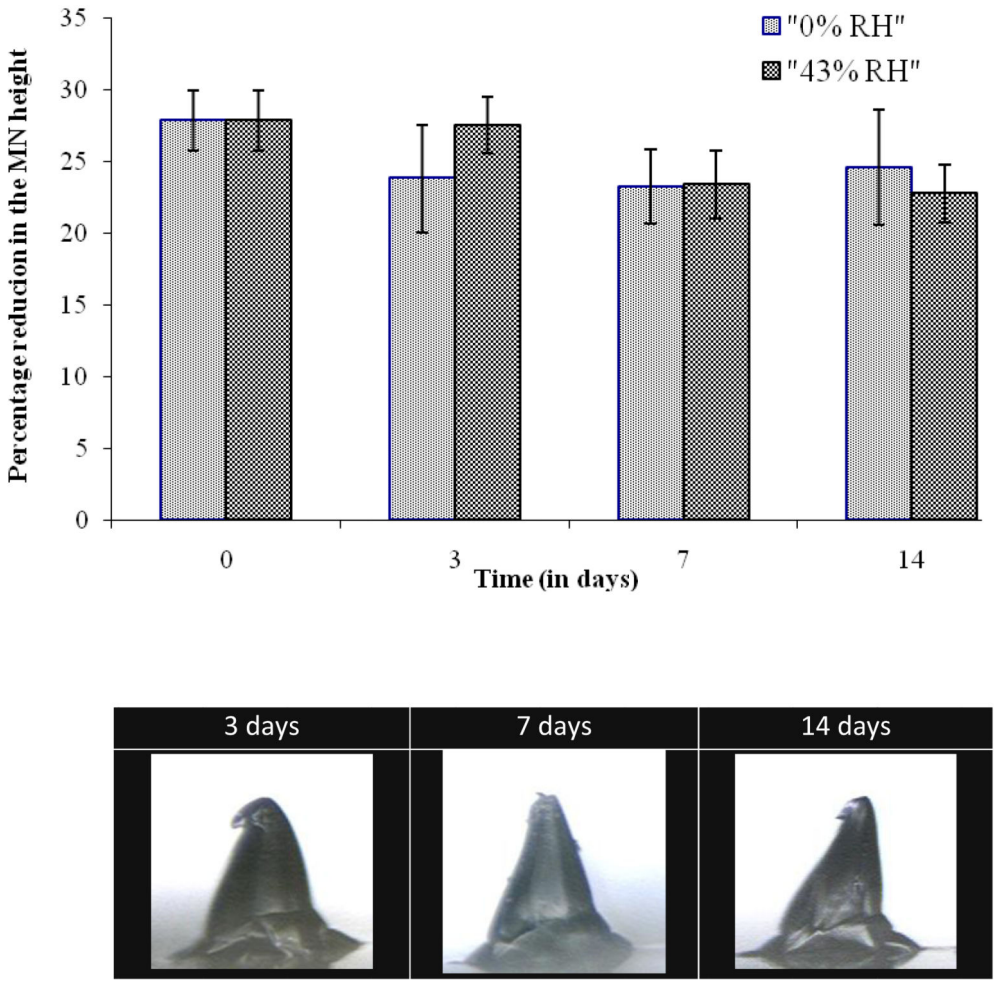

Figure 10.

Percentage reduction in the height of microneedle arrays under an axial load of 0.2 N per needle after storing at 0% RH and 43% RH for different time intervals (means ±SD, N = 6) (A) and representative digital microscope images of microneedles stored at 86% RH (B).

Europe PMC Funders Author Manuscripts

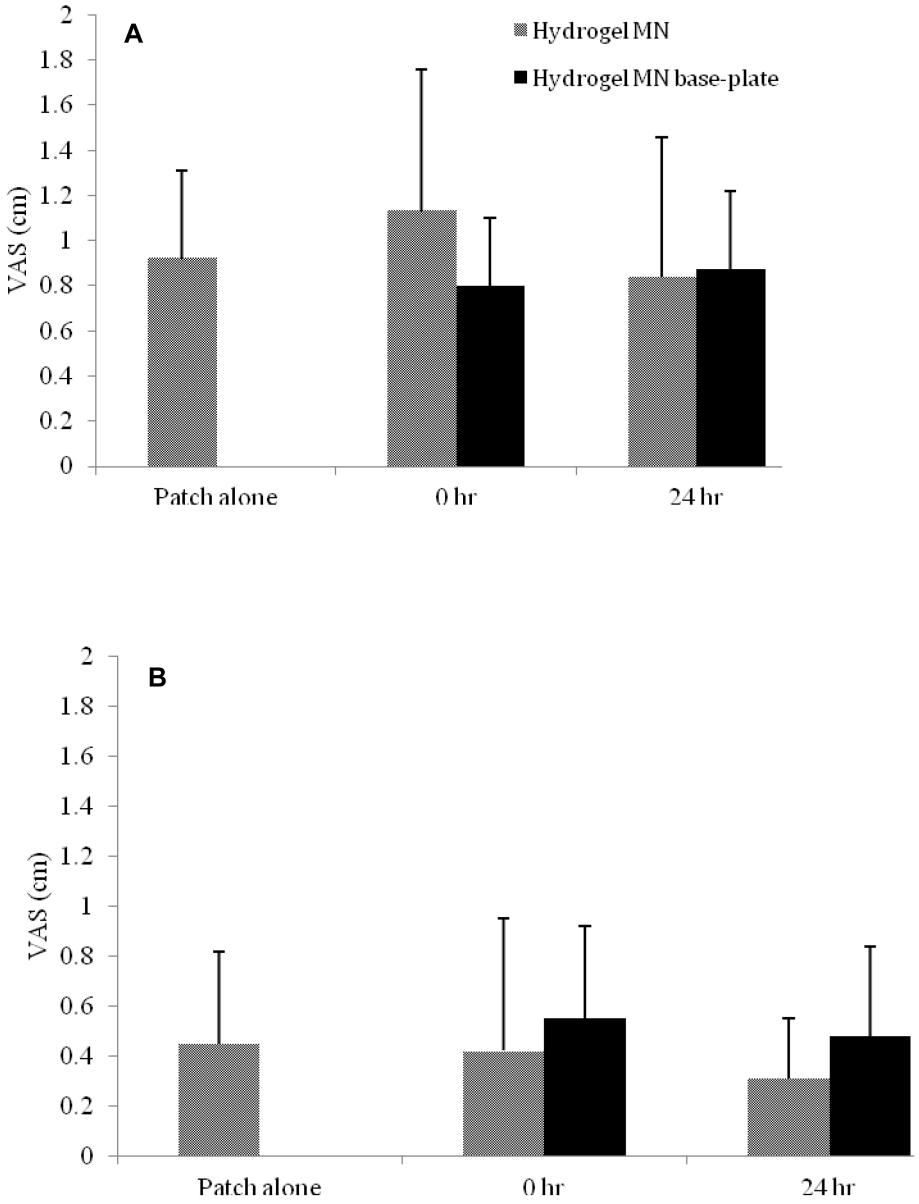

Figure 11.
VAS scores measured following (A) immediately after application of patches (B) immediately after removal of patches.

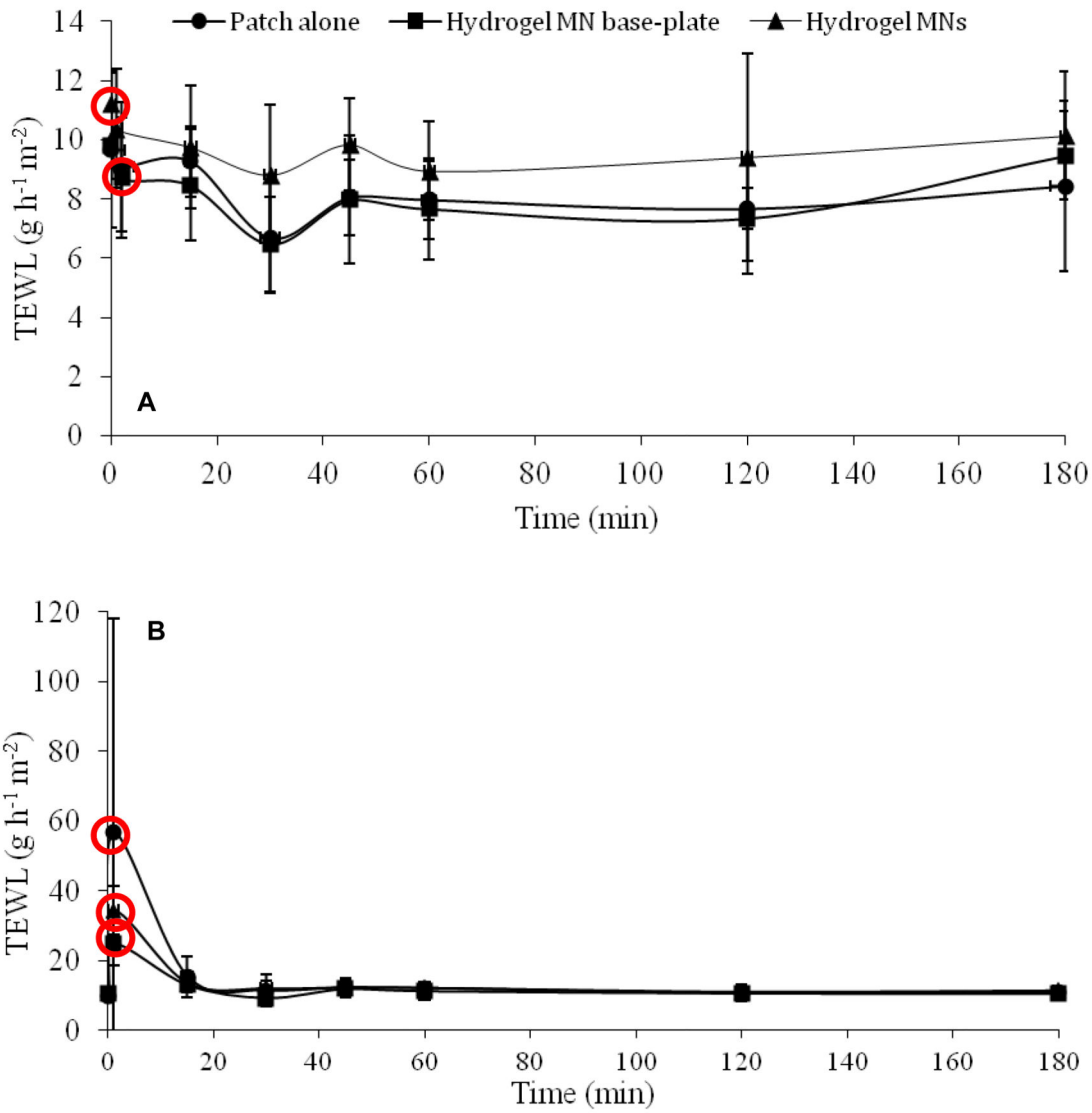

Figure 12.

Transepidermal water loss (TEWL) values measured before applying and after removing in a (A) 0 hr and (B) 24 hrs treatment protocol (means ± SD, N=6). The red circles indicate the TEWL measurements measured immediately after removing the respective patches.

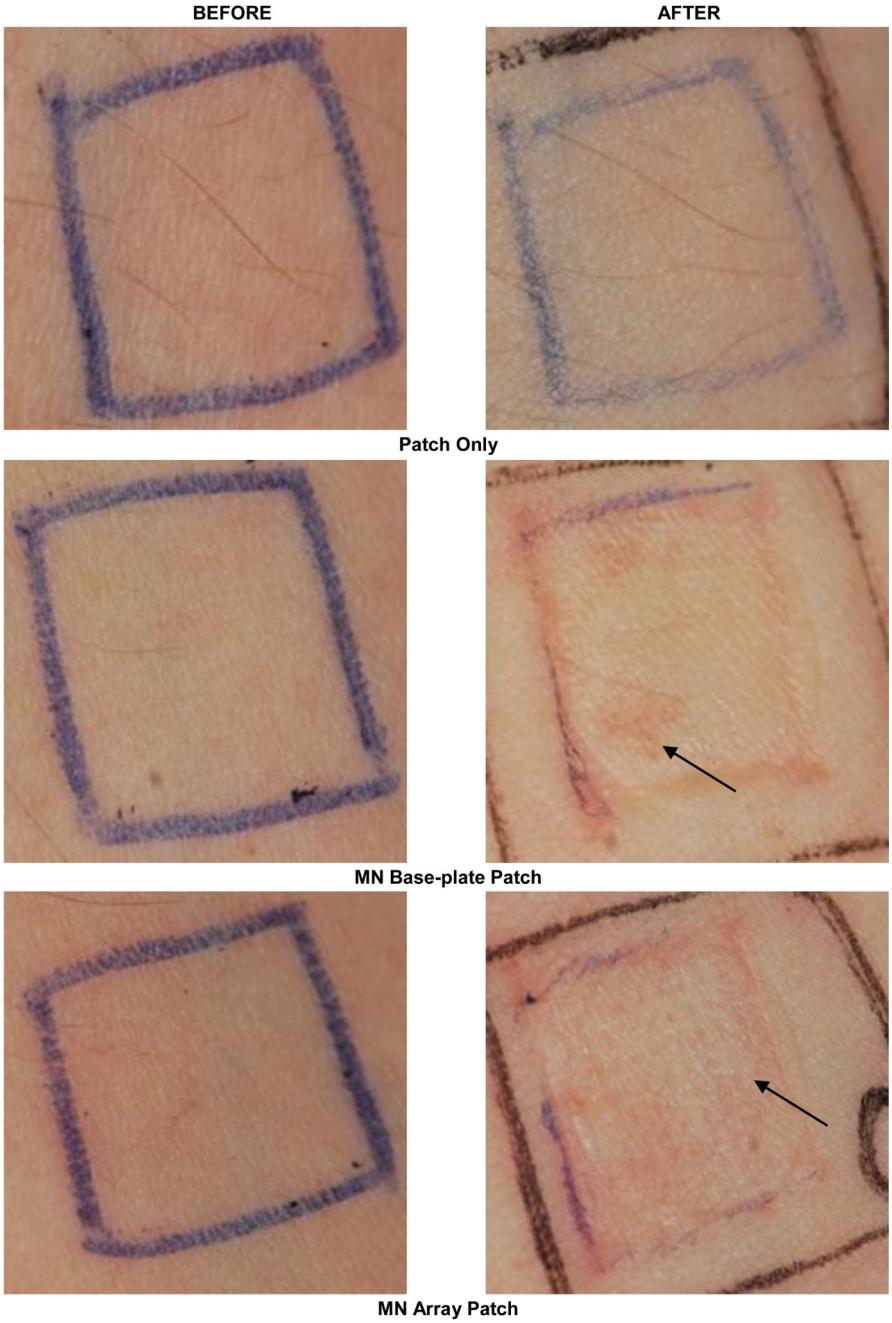

Figure 13.

Clinical photographs taken by digital camera in a 24 hr treatment protocol. Photographs on the left-hand side were taken before application of respective patches and on the right-hand side shows removal of respective patches after 24 hrs. Arrow indicates redness of skin and micro-conduits following microneedle array piercing.

Europe PMC Funders Author Manuscripts

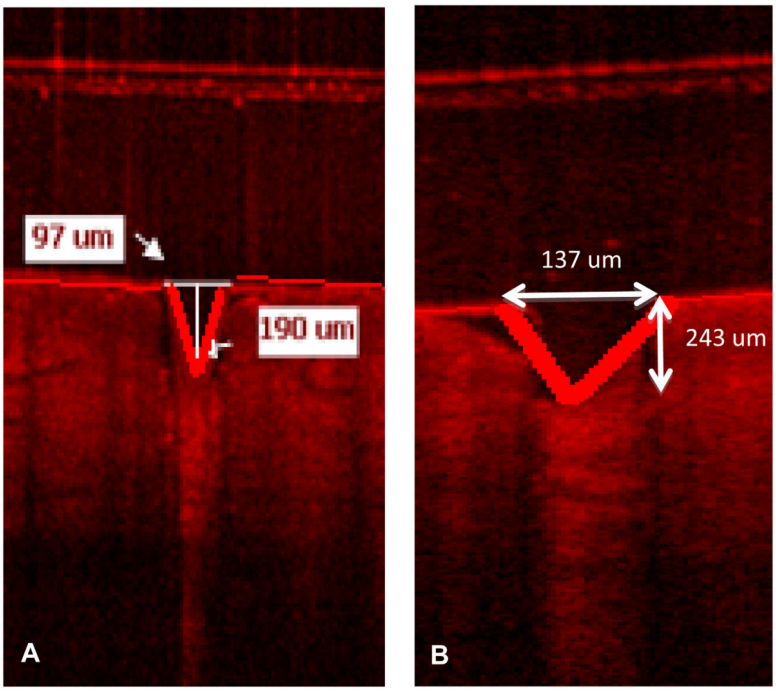

Figure 14.

OCT images of *in vivo* swelling of hydrogel-forming microneedles over 24 hours. Images show were taken at 0 (A) and time = 24 hours(B).

Europe PMC Funders Author Manuscripts

Table 1

Folding endurance (FE) of the MN base-plates stored in different RH and analyzed at different time intervals. "+" *indicates that the FE was ZERO and "−" indicates that the FE was greater than ZERO.*

FE analyzed at different days	0% RH	43% RH	86% RH
	F2	F2	F2
0	+	+	+
3	+	+	−
7	+	+	−
14	+	+	−
21	+	+	−

Table 2

A criteria of acceptance for evaluation of preservative efficacy test in terms of the log reduction in the number of viable micro-organism against the value obtained from the inoculum

		Log reduction			
		2days	**7days**	**14days**	**28days**
Bacteria	A	2	3	-	No increase
	B	-	-	3	No increase
Fungi	A	-	-	2	No increase
	B	-	-	1	No increase

The A criteria express the recommended efficacy to be achieved. In justified cases where the A criteria cannot be attained, for example for reasons of an increased risk of adverse reactions, the B criteria must be satisfied.

Europe PMC Funders Author Manuscripts

Table 3A

Total Viable Count Results for the Test for Preservation for *S.aureus* Suspension

S.aureus	**Time**	**0 day CFU/MN**	**2days CFU/MN**	**7days CFU/MN**
		4.8×10^5	-	-
		1.4×10^6	-	-
F2	A	4.8×10^5	-	-
	B	1.4×10^5	-	-

Europe PMC Funders Author Manuscripts

Table 3B

Total Viable Count Results for the Test for Preservation for *P.aeruginosa* Suspension

P.aeruginosa	**Time**	**0 day CFU/MN**	**2days CFU/MN**	**7days CFU/MN**
		0.8×10^5	-	-
		2.4×10^5		
F2	A	0.8×10^5	-	-
	B	2.4×10^5		

Europe PMC Funders Author Manuscripts

Table 3C

Total Viable Count Results for the Test for Preservation for *A.brasiliensis* Suspension

A.brasiliensis	**Time**	**0 day CFU/MN**	**2days CFU/MN**	**7days CFU/MN**	**14days CFU/MN**
		2.9×10^5	-	-	-
		2.9×10^5	-	-	-
F2	A	2.9×10^5	-	-	-
	B	2.9×10^5	-	-	

Europe PMC Funders Author Manuscripts

Table 3D

Total Viable Count Results for the Test for Preservation for *C.albicans* Suspension

C.albicans	Time	0 day CFU/aliquot of gel used to prepare MN	2days CFU/MN	7days CFU/MN	14days CFU/MN
F1	A	2.1×10^5	-	-	-
	B	2.1×10^5	-	-	-
F2	A	2.1×10^5	-	-	-
	B	2.2×10^5	-	-	-

Table 4

Influence of puncture protocol on the number of microorganisms found on the *stratum corneum* or in the viable tissue of neonate porcine skin, on the number of microorganisms completely traversing the skin to the receptor fluid in the receiver compartments of the Franz cells and comparison of these numbers with the number of MO found on unpunctured *stratum corneums*.

		Total viable count of microorganisms (CFU) found in: (% of original count on control *stratum corneum*)		
Treatment	**Microorganism**	***Stratum corneum***	**Viable tissue**	**Receptor fluid**
Control	*C. albicans*	$1.7 \pm 0.3 \times 10^7$	ND	ND
	P. aeruginosa	$5.9 \pm 1.2 \times 10^7$	ND	ND
	S. epidermidis	$3.6 \pm 0.4 \times 10^7$	ND	ND
Needle	*C. albicans*	$5.8 \pm 1.4 \times 10^6$ (38.67%)	$9.7 \pm 2.2 \times 10^4$ (0.65%)	$7.2 \pm 0.6 \times 10^6$ (48.00%)
	P. aeruginosa	$3.1 \pm 2.7 \times 10^7$ (44.29%)	ND	ND
	S. epidermidis	$2.2 \pm 0.5 \times 10^7$ (59.46%)	$3.1 \pm 0.9 \times 10^5$ (0.84%)	$1.3 \pm 0.6 \times 10^6$ (3.51%)
Left	*C. albicans*	$2.8 \pm 0.2 \times 10^6$ (16.47%)	$1.3 \pm 0.4 \times 10^5$ (0.76%)	ND
	P. aeruginosa	$3.1 \pm 1.3 \times 10^7$ (52.54%)	ND	ND
	S. epidermidis	$0.8 \pm 0.3 \times 10^7$ (22.22%)	$2.2 \pm 1.1 \times 10^5$ (1.29%)	ND
Removed	*C. albicans*	$4.2 \pm 0.2 \times 10^6$ (25.00%)	$3.6 \pm 0.3 \times 10^5$ (2.12%)	ND
	P. aeruginosa	$4.9 \pm 1.3 \times 10^7$ (83.05%)	ND	ND
	S. epidermidis	$2.6 \pm 0.7 \times 10^7$ (72.22%)	$3.8 \pm 1.0 \times 10^5$ (0.06%)	ND

ND = No microorganisms detectable. *P. aeruginosa* did not take up the radiolabel to the same extent as the other microorganisms, thus compromising experiments using it.

Europe PMC Funders Author Manuscripts

Table 5

Clinical scoring of clinical photographs by expert observers from individual volunteer's ventral forearm following respective treatment protocols.

Clinical photographs taken at:	Volunteer					
	1	2	3	4	5	6
0 hr treatment						
Patch only	0	0.5	0	0	0	0
Patch containing MN base-plate	0.5	0.5	1	0	0.5	0.5
Patch containing MN array	2	1	1	2	1	1
24 hr treatment						
Patch only	0	1	0	0	0	0
Patch containing MN base-plate	1	1	1	1	1	1
Patch containing MN array	1	2	2	1	3	1